Title

Activity of a first-in-class oral HIF2-alpha inhibitor, PT2385, in patients with first recurrence of glioblastoma.

Journal

Journal of Neuro-Oncology, 165(1)

Authors

Raymond, Catalina
Yao, Jingwen
Wen, Patrick
et al.

Publication Date

2023-10-01

DOI

10.1007/s11060-023-04456-7

Peer reviewed

HHS Public Access

Author manuscript

J Neurooncol. Author manuscript; available in PMC 2024 February 13.

Published in final edited form as:

J Neurooncol. 2023 October ; 165(1): 101–112. doi:10.1007/s11060-023-04456-7.

Activity of a first–in–class oral HIF2–alpha inhibitor, PT2385, in patients with first recurrence of glioblastoma

Roy Strowd[1], **Benjamin Ellingson**[2], **Catalina Raymond**[2], **Jingwen Yao**[2], **Patrick Y. Wen**[3], **Manmeet Ahluwalia**[4], **Anna Piotrowski**[5], **Arati Desai**[6], **Jennifer L. Clarke**[7], **Frank S. Lieberman**[8], **Serena Desideri**[9], **L. Burt Nabors**[10], **Xiaobu Ye**[11], **Stuart Grossman**[11]

[1]Wake Forest University School of Medicine, 1 Medical Center Boulevard, Winston Salem, NC 27104, USA

[2]University of California Los Angeles, Los Angeles, CA, USA

[3]Dana-Farber Cancer Institute, Boston, MA, USA

[4]Cleveland Clinic, Cleveland, OH, USA

[5]Memorial Sloan Kettering Cancer Center, New York, NY, USA

[6]University of Pennsylvania, Philadelphia, PA, USA

[7]University of California San Francisco, San Francisco, CA, USA

[8]University of Pittsburgh, Pittsburgh, PA, USA

[9]Johns Hopkins Hospital, Baltimore, MD, USA

✉Roy Strowd, rstrowd@wakehealth.edu.

Author contributions RES and SG initially conceptualized the study. RES, XY, SD, LBN, PYW, and SG designed the study.RES and SD wrote and designed the study protocol.BE, CR, and JY developed, designed, and implemented exploratory imaging analysis.RES, PYW, MA, AP, AD, JLC, FSL, LBN and SG conducted the study.XY conducted the analysis of study data.BE, CR and JY conducted the analysis of exploratory imaging data.RES, XY, BE, JY, and SG prepared the tables and figures.RES, XY, and BE wrote the first draft of the manuscript.All authors edited, reviewed, and approved the final version of the manuscript.

Supplementary Information The online version contains supplementary material available at https://doi.org/10.1007/s11060-023-04456-7.

Clinicaltrials.gov identifier NCT03216499.

Declarations

Conflict of interest Dr. Roy E. Strowd serves as a consultant for Monteris Medical and Novocure. He receives an editorial stipend from the American Academy of Neurology. He has received research/grant support from the American Academy of Neurology, American Society for Clinical Oncology, Southeastern Brain Tumor Foundation, Jazz Pharmaceuticals, and the International Association for Medical Science Educators. He receives royalties from Elsevier, Lecturio and Kaplan Medical. Dr. Benjamin Ellingson, Ms. Catalina Raymond, Dr. Jingwen Yao, Dr. Anna Piotrowski, Dr. Arati Desai, Dr. Frank Lieberman, Ms. Serena Desideri, Dr. Xiaobu Ye and Dr. Stuart Grossman has nothing to disclose. Dr. Patrick Wen has received research support from Astra Zeneca/Medimmune, Beigene, Celgene, Chimerix, Eli Lily, Genentech/Roche, Kazia, MediciNova, Merck, Novartis, Nuvation Bio, Puma, Servier, Vascular Biogenics, VBI Vaccines and serves on advisory boards for Astra Zeneca, Bayer, Black Diamond, Boehringer Ingelheim, Boston Pharmaceuticals, Celularity, Chimerix, Day One Bio, Genenta, Glaxo Smith Kline, Karyopharm, Merck, Mundipharma, Novartis, Novocure, Nuvation Bio, Prelude Therapeutics, Sapience, Servier, Sagimet, Vascular Biogenics, and VBI Vaccines. Dr. Manmeet Ahluwalia receives grants/research support from Astrazeneca, BMS, Bayer, Incyte, Pharmacyclics, Novocure, Mimivax, and Merck, consults for Bayer, Novocure, Kiyatec, Insightec, GSK, Xoft, Nuvation, Cellularity, SDP Oncology, Apollomics, Prelude, Janssen, Tocagen, Voyager Therapeutics, Viewray, Caris Lifesciences, Pyramid Biosciences, AnHeart Therapeutics, Varian Medical Systems, and Cairn Therapeutics, is on the Scientific Advisory Board for Cairn Therapeutics and Pyramid Biosciences, and is a stock shareholder for Mimivax, Cytodyn, MedInnovate Advisors LLC. Dr. Jennifer Clarke has served as consultant for Servier Pharmaceuticals and Agios Pharmaceuticals. Research support from Servier Pharmaceuticals, Agios Pharmaceuticals, and Merck & Co. Dr. L. Burt Nabros, MD serves on scientific advisory board for Chimerix and chairs the data safety monitoring committee for CNS Pharma. M.P. has consulted for Bayer, is a member of the HI-TRON Scientific Management Board and holds patents for peptides for use in treating or diagnosing IDH1R132H positive cancers (EP2800580B1).

[10]University of Alabama at Birmingham, Birmingham, AL, USA

[11]Sidney Kimmel Comprehensive Cancer Center, Johns Hopkins, Baltimore, MD, USA

Abstract

Introduction—Hypoxia inducible factor 2-alpha (HIF2α) mediates cellular responses to hypoxia and is over-expressed in glioblastoma (GBM). PT2385 is an oral HIF2α inhibitor with in vivo activity against GBM.

Methods—A two-stage single-arm open-label phase II study of adults with GBM at first recurrence following chemoradiation with measurable disease was conducted through the Adult Brain Tumor Consortium. PT2385 was administered at the phase II dose (800 mg b.i.d.). The primary outcome was objective radiographic response (ORR = complete response + partial response, CR + PR); secondary outcomes were safety, overall survival (OS), and progression free survival (PFS). Exploratory objectives included pharmacokinetics (day 15 C_{min}), pharmacodynamics (erythropoietin, vascular endothelial growth factor), and pH-weighted amine-chemical exchange saturation transfer (CEST) MRI to quantify tumor acidity at baseline and explore associations with drug response. Stage 1 enrolled 24 patients with early stoppage for ≤ 1 ORR.

Results—Of the 24 enrolled patients, median age was 62.1 (38.7–76.7) years, median KPS 80, MGMT promoter was methylated in 46% of tumors. PT2385 was well tolerated. Grade ≥ 3 drug-related adverse events were hypoxia (n = 2), hyponatremia (2), lymphopenia (1), anemia (1), and hyperglycemia (1). No objective radiographic responses were observed; median PFS was 1.8 months (95% CI 1.6–2.5) and OS was 7.7 months (95% CI 4.9–12.6). Drug exposure varied widely and did not differ by corticosteroid use (p = 0.12), antiepileptics (p = 0.09), or sex (p = 0.37). Patients with high systemic exposure had significantly longer PFS (6.7 vs 1.8 months, p = 0.009). Baseline acidity by pH-weighted CEST MRI correlated significantly with treatment duration (R^2 = 0.49, p = 0.017). Non-enhancing infiltrative disease with high acidity gave rise to recurrence.

Conclusions—PT2385 monotherapy had limited activity in first recurrent GBM. Drug exposure was variable. Signals of activity were observed in GBM patients with high systemic exposure and acidic lesions on CEST imaging. A second-generation HIF2α inhibitor is being studied.

Keywords

Glioblastoma; Hypoxia; Hypoxia-inducible factor; Amine imaging

Introduction

Patients with glioblastoma (GBM) continue to have among the poorest prognosis of most solid tumors [1–4]. Standard of care treatment includes maximal safe surgery followed by chemoradiotherapy with temozolomide [5]. When tumors progress after first line therapy, limited options exist. Lomustine or bevacizumab is often used for salvage treatment but has limited activity in the majority of patients [5, 6]. Several recent phase II and phase III studies evaluating novel agents have failed in patients with newly diagnosed and recurrent

GBM including nivolumab, pembrolizumab, rindopepimut, and others [7–9]. New agents are needed that target novel mechanisms for this highly aggressive and lethal cancer.

Hypoxia is a fundamental process in gliomagenesis. It is strongly linked to malignant tumor behavior by driving cell proliferation, promoting angiogenesis, enhancing migration, and facilitating resistance to chemoradiation [10–14]. The hypoxia inducible factors (HIFs) are a family of transcription factors that mediate the cellular response to hypoxia. The first HIF described in the literature was HIF1-alpha (HIF1α) which was identified as a regulator of the erythropoietin (*EPO*) gene. Subsequently, the family of HIFs including HIF2α and HIF3α [15–17] have been recognized as central mediators of the cellular response to hypoxia [18, 19].

HIFs have been shown to be critical for mediating cell metabolism under hypoxia, shifting glucose metabolism from oxidative phosphorylation to glycolysis [20, 21], resulting in accumulation of lactic acid and acidification of the tumor microenvironment [22]. Tumor acidity resulting from both hypoxia and high metabolic demand further drives tumor progression [23, 24], including increasing expression of vascular endothelial growth factor (VEGF) and platelet derived growth factor (PDGF) [25, 26], leading to increased hypoxia through angiogenesis and ultimately higher expression of HIFs. HIF2α, in particular, is upregulated in GBM exposed to an acidic microenvironment [27], suggesting tumors with high acidity may benefit from HIF2α inhibition. Using pH-weighted amine chemical exchange saturation transfer (CEST) MRI, a strong association between HIF1α expression and tumor acidity as well as cerebral blood volume and tumor acidity were recently demonstrated in human IDH mutant gliomas [28, 29]. Thus, pH-weighted MRI may be useful as an enrichment biomarker for identifying tumors with high acidity, indirectly suggesting high HIF2α expression.

To date, targeting HIFs in oncology has shown promise in renal cell carcinoma and von Hippel Lindau and has not been fully explored in neuro-oncology [30]. HIF1α is ubiquitously expressed in both tumor and normal tissue limiting its therapeutic specificity [31, 32]. HIF2α appears to be a more attractive target as (1) its expression is more specific to tumor tissues, and (2) it mediates states of chronic hypoxia found in tumors [33]. In gliomas, HIF2α is expressed in glioma cells but not in normal neural progenitors or glia [34, 35] and may be clinically relevant as HIF2α expression in the REMBRANDT glioma database (n = 834) showed higher HIF2α expression in tumors that was correlated with worsened patient survival [34]. HIF2α protein expression by immunohistochemistry correlates with increasing glioma grade. We have previously shown that HIF2α was present in none of 4 grade II gliomas, 27% of 11 grade III gliomas, and 64% of 42 GBMs where expression was increased in both perinecrotic and perivascular niches (Supplementary Fig. 1) [36].

Despite the hypothetical merits of HIF2α as a therapeutic target in gliomas, translational investigations have been limited by the lack of clinically applicable inhibitors. In recent years, PT2385 was successfully developed as a first-in-class, orally available small molecule HIF2α transcriptional inhibitor [33, 37]. Initial studies of PT2385 in advanced renal cell carcinoma (RCC) with *VHL* mutations have shown promising disease activity in both

phase I and II trials. The agent is currently being studied in phase III clinical trials in RCC [38, 39]. Ongoing drug development has resulted in a second-generation compound (i.e., belzutifan) that was recently FDA-approved for the treatment of tumors in patients with von-Hippel Lindau syndrome [30]. PT2385 is an attractive agent for studying for gliomas. It is a small, lipophilic compound with favorable blood brain barrier permeability in preclinical models including a brain:plasma ratio of 0.9 in rats and 0.5 in dogs (Personal Communication, Peloton Therapeutics). Preclinical studies have demonstrated signal-agent activity in patient-derived in vitro and in vivo models of glioma [35, 36]. Furthermore, studies show that silencing HIF2α reduces neurosphere formation which complements temozolomide-based chemotherapy treatment and that this is mediated by CD44 [40, 41].

The aim of this study was to determine the efficacy, safety, and pharmacokinetic properties of the first-in-class HIF2α inhibitor, PT2385, administered as monotherapy in patients with glioblastoma at first recurrence. Additionally, we explored whether there was an association between baseline tumor acidity and PT2385 activity using pH-weighted amine CEST MRI contrast in a subset of patients.

Methods

Trial design

ABTC 1602 is a multicenter single-arm, open-label phase II study conducted within the Adult Brain Tumor Consortium (ABTC) which was designed to study the efficacy of single-agent PT2385 in patients with first recurrence of GBM.

Objectives

The primary objective was to estimate the efficacy of PT2385 as measured by radiographic response rate in patients with first recurrence of GBM. Secondary objectives included to estimate the efficacy of PT2385 as measured by progression free and overall survival; and to determine the safety in patients with recurrent glioblastoma. Exploratory objectives were to (1) describe the pharmacokinetic and pharmacodynamics properties of PT2385 and (2) describe baseline intratumoral acidity using non-invasive magnetic resonance imaging.

Participants

Participants were age 18 years or older with histologically confirmed GBM that had progressed or recurred for the first time following initial radiation and temozolomide chemotherapy, with measurable disease (defined as a contrast-enhancing lesion with a minimal square diameter of 10 mm), and who had not previously received anti-VEGF therapy (e.g. bevacizumab). Surgery at the time of recurrence was permitted but not required. Participants not receiving surgery were required to have unequivocal radiographic evidence of recurrence according to the Response Assessment in Neuro-Oncology (RANO) criteria [42]. Additional exclusion criteria were bleeding diathesis, concurrent treatment with enzyme-inducing anti-epileptic drugs (EIAEDs), uncontrolled intercurrent illness, or participants with known infection with human immunodeficiency virus. Participants were not excluded by molecular profiling but results of clinically available testing was required for isocitrate dehydrogenase (IDH) gene testing and O(6)-methylguanine-

DNA-methyltransferase (MGMT) methylation testing. Participants were required to have recovered from toxicity of prior therapy, be without prior malignancy for ≥ 5 years, and have acceptable organ and marrow function including hemoglobin ≥ 9 g/dL, platelet count ≥ 100,000/mcL and creatinine clearance > 60 mL/min/1.73 m^2 or creatinine ≤ institutional upper limit of normal (ULN).

Treatment

Following screening, participants received PT2385 at the recommended phase II dose of 800 mg twice daily continuously in 28-day cycles until progression or unacceptable toxicity. Participants received routine blood work weekly including weekly complete blood count to monitor hemoglobin as this agent has been associated with anemia due to a reduction in circulating EPO levels and weekly pulse oximetry for the first 8 weeks due to an association with asymptomatic hypoxemia. Neurological examination and magnetic resonance imaging (MRI) of the brain with and without gadolinium contrast were performed every 8 weeks for clinical and radiographic response assessment. Blood samples to characterize the plasma pharmacokinetic and pharmacodynamics of PT2385 were obtained at baseline and weeks 1, 2 and 4 of the first cycle to establish a steady-state minimum concentration (C_{min}). Participants at qualified sites (7-out-of-11 total sites) completed a one-time advanced magnetic resonance imaging study (see below) to assess tumoral acidity and hypoxia and correlate with subsequent response.

Study endpoints

The primary endpoint of the study was objective radiographic response rate defined as complete response (CR) and partial response (PR) according to RANO criteria. Imaging response was initially assessed by the treating physician; all PR and CR were confirmed by independent central review. Secondary endpoints were (1) safety according to NCI Common Terminology Criteria for Adverse Events (CTCAE), (2) overall survival (OS), and (3) progression free survival (PFS). Exploratory outcomes included pharmacokinetic (PK), pharmacodynamics (PD) parameters, and anatomic and pH-weighted amine CEST MRI imaging.

Pharmacokinetic and pharmacodynamic assessments

Blood samples for PK and PD assessment were drawn 1 h before and 6 h after PT2385 administration on day 1 of cycle 1 and 1 h before PT2385 administration on day 15 and day 1 of cycle 2 to determine steady-state concentration. These time points were selected based on experience from prior studies of this agent [33] indicated that pretreatment and 6 h-post-dose time points provide optimal assessment of trough, maximum observed plasma concentrations, and steady state (i.e., Day 15 C_{min}). Plasma concentrations of PT2385 were determined by validated liquid chromatography/mass spectrometry method. To measure target engagement, plasma EPO and VEGF concentrations were measured 1 h before and 6 h after PT2385 administration on day 1 of cycle 1 and 1 h prior to PT2385 administration on day 2 of cycle 2. EPO and VEGF were measured using the Access Immunoassay System (Beckman Coulter, Brea, CA).

Anatomic and pH–weighted amine CEST MRI

Anatomic MR images were acquired according to the standardized brain tumor imaging protocol (BTIP) [43] by all ABTC participating cites. Four ABTC sites with Siemens 3 T MR systems (Trio, Skyra, or Prisma, Siemens Healthcare; Erlangen, Germany) participated in the advanced imaging component of the study. Specifically, Wake Forest, University of Pennsylvania, Dana Farber Cancer Institute, and Johns Hopkins University participated; each institute used either a previously described amine CEST echoplanar (CEST-EPI) [44] or amine CEST spin-and-gradient-echo echoplanar (CEST-SAGE-EPI) sequence [45]. CEST MR acquisition parameters included a field-of-view (FOV) = 240 × 217 mm, matrix size = 128 × 116, slice thickness = 4 mm with no interslice gap, TE = 27 ms for single-echo CEST-EPI and 14.0 ms and 34.1 ms for the two gradient echoes using CEST-SAGE-EPI, bandwidth = 1628 Hz, and GRAPPA factor = 2 for single-echo CEST-EPI and 3 for CEST-SAGE-EPI. Off-resonance saturation was applied using a pulse train of 3 × 100 ms Gaussian pulses with peak amplitude of 6μT. A total of 29 off-resonance frequencies were sampled at − 3.5 to − 2.5 ppm, − 0.3 to + 0.3 ppm, and + 2.5 to + 3.5 ppm, with increments of 0.1 ppm. A reference S_0 scan was collected with the same acquisition parameters, without the saturation pulses. The total scan time for CEST was approximately 7.5 min.

All CEST-SAGE-EPI and CEST-EPI images were motion corrected using an affine transformation (*mcflirt*; FSL, FMRIB, Oxford, United Kingdom) and B_0 correction via a *z*-spectra based *k*-means clustering and Lorentzian fitting algorithm [46]. Following motion and B_0 correction, the integral of width of 0.4 ppm was quantified around both the − 3.0 and + 3.0 ppm (− 3.2 to − 2.8 ppm and + 2.8 to + 3.2 ppm, respectively) spectral points. These data points were combined with the S_0 image to calculate the asymmetry in the magnetization transfer ratio (MTR_{asym}) at 3.0 ppm, a measure related to pH [45], as defined using equation: $MTR_{asym}(3.0\,\text{ppm}) = S(-3.0\,\text{ppm})/S_0 - S(+3.0\,\text{ppm})/S_0$, where $S(\omega)$ is the amount of bulk water signal available after the saturation pulse with offset frequency ω and S_0 is the signal available without application of RF saturation. For CEST-SAGE-EPI data, the average MTR_{asym} at 3.0 ppm calculated by averaging the first (TE = 14.0 ms) and second (TE = 34.1 ms) gradient echoes to increase the available signal-to-noise. MTR_{asym} was calculated for both contrast enhancing tumor and peritumoral edema defined by T2 hyperintensity on FLAIR images. All post-processing was performed with MATLAB (Release 2017b, MathWorks, Natick, MA). All resulting maps were registered to high-resolution post-contrast T1-weighted images for subsequent analyses.

Statistical analysis

The primary objective of this study was to estimate tumor response rate. The data analysis was based intent-to-treat population. Safety analysis was performed on participants who received at least one dose of study drug. Data were presented with standard descriptive summaries. Response rate was presented as percentage along with 95% confidence interval (exact method). Observed toxicities were summarized based on CTCAE v5.0 with relationship of possible, probable, and definitely to the treatment. Survival and progression-free probabilities were estimated using the Kaplan–Meier method. The confidence interval of median time survival was constructed by the method of Brookmeyer-Crowley (Brookmeyer, 1982). Pharmacokinetic and pharmacodynamics analysis were performed to

estimate the minimum circulating concentration at day 15 (PK only, D15 C_{min}) and day 29 (PK and PD). The correlation between drug exposure, target engagement was assessed using Pearson correlation coefficient. The Log-rank statistics were used to explore an association between the drug exposure to progression-free survival. All analyses were conducted using the SAS software (version 9.3, SAS Institute).

Sample Size

A minimum of 24 patients and maximum of 35 participants was estimated based on a two-stage design (MINIMAX) with 85% statistical power and a false positive rate of 5%. The primary endpoint was objective radiographic response rate (CR + PR). The study hypothesized that single-agent PT2385 would achieve at least a 20% response rate which was considered clinically meaningful compared to a null hypothesis of 5%. A response rate of ≤ 1 in 24 patients enrolled in stage 1 was determined to meet early stoppage criteria for futility. Otherwise, the study would enroll a total of 35 participants to complete stage 2. The probability of early stopping for futility was 0.661 when the null was true and 0.033 when a true response is 20%.

Ethics

The protocol was approved by the institutional review boards (IRBs) at all participating institutions and registered at clinicaltrials.gov (NCT03216499). The study protocol was developed by the principal investigator and ABTC staff. The clinical database was maintained and controlled by the ABTC. All clinical data were collected and reviewed by the ABTC staff and principal investigator. Statistical analysis was performed by the ABTC statistician (X.Y.).

Results

Patient population

Between September 2017 and March 2018, 24 participants were enrolled. Baseline characteristics were consistent with those expected in this population with median age 62.1 (38.7–76.7) years, 63% male, 92% white, 4% black and 4% race not reported (Tables 1, 2). MGMT promoter was reported to be methylated in 46%, not methylated in 50% and indeterminant in 4%. Extent of resection at the time of initial diagnosis was gross total resection in 58%. All patients had previously received radiation therapy and temozolomide chemotherapy. Median performance status at the time of study enrollment was 80 (range 70–100). Corticosteroids were prescribed for 38% of patients at enrollment.

Pharmacokinetics and pharmacodynamics

Substantial variability in drug exposure was observed. Mean day 15 C_{min} concentration (D15 C_{min}) was 393 ± 424 ng/mL. The majority of patients (55%) had D15 C_{min} < 300 ng/mL; 25% of patients had D15 C_{min} 300–1000 ng/mL; and in 3 patients (15%) D15 C_{min} was ≥ 1000 ng/mL (Fig. 1). Drug exposure did not differ by corticosteroid use ($p = 0.12$), antiepileptics ($p = 0.09$), or sex ($p = 0.37$).

The mean change in EPO was − 4.8 (± 7.7, p = 0.029) 6-h following initial PT2385 administration on day 1 of cycle 1 and − 5.5 (± 6.7, p = 0.007) at steady state 1-h prior to PT2385 administration on day 1 of cycle 2 (Supplementary Fig. 2). There was no significant change in serum VEGF concentrations on day 1 at 6-h post-dose (− 9.5, ± 22.4, p = 0.172) or day 1 of cycle 2 (10.1, ± 41.6, p = 0.486). There was a strong correlation between higher serum VEGF concentrations at the 6-h post-dose on day 1 and D15 C_{min} (R^2 = 0.65, p = 0.009). This correlation was not observed after steady state was achieved at day 1 of cycle 2 (R^2 = − 0.23, p = 0.444, Supplementary Fig. 2).

Efficacy

Of the 24 patients evaluable for efficacy, no objective radiographic responses were observed. The best response was stable disease in 7 patients (29%, 95% CI 13–51%) and progressive disease in 17 (71%, 95% CI 49–87%). Progressive disease was defined by imaging for 15 patients (68%) and imaging plus clinical deterioration for 7 patients (32%). One patient discontinued treatment due to toxicity and one other discontinued treatment due to physician's choice. The trial met criteria for early stoppage for futility.

Median duration on treatment was 2.0 months (95% CI 1.3–3.1, Fig. 2). Median progression free survival for the entire cohort was 1.8 months (95% CI 1.6–2.5). Median overall survival was 7.7 months (95% CI 4.9–12.6, Fig. 2). At the time of database lock, 21 out of 24 patients had died. Twenty-one patients experienced tumor recurrence and one patient had a new lesion at the time of disease progression. Salvage treatment included bevacizumab or bevacizumab plus another chemotherapy for 12 patients, lomustine for 3, and one patient received reirradiation with temozolomide.

Patients with the highest systemic exposure had significantly longer progression free survival (6.7 vs 1.8 months, 0.009, Table 3 & Fig. 1)). While patients with intermediate or lower systemic exposure (i.e., D15 C_{min} < 1000 ng/mL) progressed rapidly, duration on treatment was considerably longer for three patients the highest systemic exposure (i.e., D15 C_{min} > 1000 ng/mL). These three tumors included 2 MGMT unmethylated and 1 MGMT methylated IDH wild type glioma including one patient with biopsy proven recurrence at 7 months following completion of chemoradiation whose imaging showed progressive tumor growth prior to treatment initiation which stabilized on drug (Fig. 3).

Safety

All 24 patients were evaluable for safety. In general, PT2385 was well tolerated. One grade 4 lymphopenia was observed. Grade 3 adverse events included hypoxia (n = 2), hyponatremia (2), anemia (1), and hyperglycemia (1). The most common adverse event was grade 1 asymptomatic anemia. Other adverse events attributed to PT2385 are reported in Table 2.

pH–weighted amine CEST MRI

pH-weighed CEST imaging was completed at baseline in 11 patients including 2 patients with high systemic drug exposure (D15 C_{min} > 1000 ng/mL), 2 patients with intermediate exposure (D15 C_{min} 300–1000 ng/mL), and 7 with low exposure (D15 C_{min} < 300 ng/mL). Higher baseline acidity by pH-weighted CEST correlated with greater duration on treatment

(R^2 = 0.49) and drug exposure (R^2 = 0.64) in non-enhancing peritumoral regions and not in enhancing tumor (Fig. 4). Patients whose lesions that were more acidic at baseline remained on drug the longest. This was the case for non-enhancing disease but not the necrotic central enhancing regions. Patients who had acidic lesions at baseline also tended to be those with greater systemic exposure, which may confound this effect. Additionally, localized regions with high acidity at baseline appeared to predict future areas of treatment failure (Supplementary Fig. 3), similar to previous reports in bevacizumab treatment [28].

Discussion

This is the first trial to report the clinical activity of a small molecular inhibitor of HIF2α in patients with recurrent GBM. The primary efficacy endpoint was not met as no objective radiographic responses were observed and the study met early stopping criteria for futility. This study has three important findings including that (1) PT2385 was safe, well tolerated, and had an expected side effect profile and on-target inhibition in patients with first recurrence of GBM, (2) drug exposure to PT2385 was highly variable, and (3) while signals of activity were observed including that patients with higher drug exposure (i.e. $C_{min} \geq 1000$ ng/dL) had substantially longer stable disease by imaging, no disease activity was documented of single-agent treatment. In addition, this is one of the first studies to report on the incorporation of a multicenter pH-weighted advanced imaging analysis which revealed that patients with high acidity signals in non-enhancing disease at baseline (i.e. more hypoxic) had longer stable disease on treatment by imaging.

PT2385 is a first-in-class inhibitor of HIF2α, which was first studied in patients with RCC. In the initial phase 1 dose-finding study in RCC imaging responses were observed including complete response in 2%, partial response in 12%, and the majority of responders showing prolonged stable disease (52%) [33]. In this prior study, day 15 pharmacokinetic profiling showed that PT2385 (800 mg) was rapidly absorbed with median T_{max} of 2 h, mean C_{max} of 3.1 μg/mL, and mean half-life of 17 h. Significant variability was observed in drug exposure in the current study. PT2385 undergoes extensive hydroxylation, oxidative defluorination and glucuronidation in the gut with multiple hepatic CYP enzymes participating in its metabolism including CYP2C19 which plays a critical role in the metabolism of anticancer, antidepressant, antihypertensive, and antiplatelet drugs [47, 48]. Prior metabolic profiling has suggested that genetic polymorphisms of CYP2C19 and UGT2B17 may explain individual variation observed in human trials of PT2385 [47]. In the current study, day 15 C_{min} did not differ for patients prescribed corticosteroids, antiepileptics, or by patient sex. It is not known whether genetic polymorphisms present in this cohort or additional factors may have contributed to this variability.

This study did not meet its primary efficacy endpoint and enrollment was concluded for futility after stage 1. While the negative efficacy result is discouraging, this study highlights the benefit of a single-arm phase II two-stage trial design when testing novel compounds with high risk/benefit for patients with terminal cancers. This study rapidly completed enrollment in only 6 months. That speed, in combination with the significant variability in systemic drug exposure, and the determination of futility after 24 patients and only 6 months allowed the pharmaceutical drug developer to determine that further drug development was

needed. A second-generation compound, bezultifan, with more consistent drug exposure was sought and is now in clinical trials (NCT02974738).

The correlation between drug exposure and duration of stable disease is an interesting and potentially important finding. Patients in this study with low systemic drug exposure progressed rapidly by the time of initial response assessment imaging at 2 months. This included patients with both MGMT methylated and unmethylated recurrent gliomas. In contrast, patients with the highest systemic drug exposure showed a considerably different duration on treatment and stabilization of disease. While serum EPO concentrations declined significantly following PT2385 administration and at steady state, no change in circulating VEGF concentrations was observed. However, patients with higher VEGF concentrations at treatment initiation had higher drug exposure. Prior studies clinical and preclinical studies of PT2385 in patients with RCC indicate that the major action of this compound may be cytostatic as opposed to cytotoxic supporting prolonged PFS as an optimal endpoint in clinical trials of this agent [33, 35, 36]. Recent studies have suggested that acquired mutation in TP53 may lead to therapeutic resistance. Given the frequency of intrinsic TP53 mutation in glioma, this may contribute to the likelihood of response in glioma patients and requires further study [49]. Despite this, no change in circulating VEGF concentrations were observed.

This is one of the first studies to successfully implement multicenter pH-weighted CEST imaging. The finding that high acidity signals in non-enhancing disease at baseline (i.e., more metabolically abnormal) was seen in patients who had longer stable disease by imaging suggests that early incorporation of imaging biomarker assessment into clinical trials could be beneficial for drug development. In addition, the finding that patients who had acidic lesions at baseline also tended to be those with greater systemic exposure raises some interesting questions about whether the acidity on imaging could reflect differences in those patients' metabolism of PT2385. More experience with this imaging study is needed before conclusions can be drawn. The variability in systemic exposure that was observed for patients in this study was not anticipated, and this study was not designed to test whether pH-weighted imaging could be used to predict the differences in drug exposure that were observed. Further study is needed to determine whether this imaging sequence could be a predictive biomarker of response for agents in this class of drug.

The finding that high acidity in non-enhancing disease at baseline had longer stable disease by imaging supports the hypothesis that acidic tumors may have elevated HIF2α and, thus, may have some therapeutic benefit from HIF2α inhibition. In addition, the finding that patients who had acidic lesions at baseline also tended to be those with greater systemic exposure raises some interesting questions about whether the acidity on imaging could reflect differences in those patients metabolism of PT2385. At this point, more experience with this imaging study and in particular with a drug that does not demonstrate the variability in pharmacokinetics is needed to determine whether this imaging sequence could be a predictive biomarker of drug response.

In conclusion, single-agent PT2385 has acceptable safety but minimal activity in patients with first recurrence of GBM. Drug exposure to PT2385 was highly variable. Signals of

activity were observed in patients with high systemic exposure and in those with acidic lesions on pH-weighted advanced MRI imaging at baseline. A second-generation HIF2α inhibitor is currently being studied.

Supplementary Material

Refer to Web version on PubMed Central for supplementary material.

Funding

Research reported in this publication was supported by the National Institutes of Health (NIH) through Grant UM1CA137443.

References

1. Stupp R, Taillibert S, Kanner A et al. (2017) Effect of tumor-treating fields plus maintenance temozolomide vs maintenance temozolomide alone on survival in patients with glioblastoma. JAMA 318(23):2306. 10.1001/jama.2017.18718 [PubMed: 29260225]
2. Stupp R, Taillibert S, Kanner AA et al. (2015) Maintenance therapy with tumor-treating fields plus temozolomide vs temozolomide alone for glioblastoma. JAMA 314:2535. 10.1001/jama.2015.16669 [PubMed: 26670971]
3. Stupp R, Mason W, van den Bent M et al. (2005) Radiotherapy plus concomitant and adjuvant temozolomide for glioblastoma. NEJM 352(10):987–996 [PubMed: 15758009]
4. Malmström A, Grønberg BH, Marosi C et al. (2012) Temozolomide versus standard 6-week radiotherapy versus hypofractionated radiotherapy in patients older than 60 years with glioblastoma : the Nordic randomised, phase 3 trial. Lancet Oncol 13(9):916–926. 10.1016/S1470-2045(12)70265-6 [PubMed: 22877848]
5. Wen PY, Weller M, Lee EQ et al. (2020) Glioblastoma in adults: a Society for Neuro-Oncology (SNO) and European Society of Neuro-Oncology (EANO) consensus review on current management and future directions. Neuro-oncology 22(8):1073–1113. 10.1093/NEUONC/NOAA106 [PubMed: 32328653]
6. Wick W, Gorlia T, Bendszus M et al. (2017) Lomustine and bevacizumab in progressive glioblastoma. N Engl J Med 377(20):1954–1963. 10.1056/NEJMOA1707358/SUPPL_FILE/NEJMOA1707358_DISCLOSURES.PDF [PubMed: 29141164]
7. Weller M, Butowski N, Tran DD et al. (2017) Rindopepimut with temozolomide for patients with newly diagnosed, EGFRvIII-expressing glioblastoma (ACT IV): a randomised, double-blind, international phase 3 trial. Lancet Oncol 18(10):1373–1385. 10.1016/S1470-2045(17)30517-X [PubMed: 28844499]
8. Reardon DA, Kim TM, Frenel JS et al. (2021) Treatment with pembrolizumab in programmed death ligand 1-positive recurrent glioblastoma: results from the multicohort phase 1 KEY-NOTE-028 trial. Cancer 127(10):1620–1629. 10.1002/CNCR.33378 [PubMed: 33496357]
9. Reardon DA, Brandes AA, Omuro A et al. (2020) Effect of nivolumab vs bevacizumab in patients with recurrent glioblastoma: the checkmate 143 phase 3 randomized clinical trial. JAMA Oncol 6(7):1003–1010. 10.1001/JAMAONCOL.2020.1024 [PubMed: 32437507]
10. Axelson H, Fredlund E, Ovenberger M, Landberg G, Pahlman S (2005) Hypoxia-induced dedifferentiation of tumor cells—a mechanism behind heterogeneity and aggressiveness of solid tumors. Semi Cell Dev Biol 16:554–563
11. Harris AL (2002) Hypoxia—a key regulatory factor in tumour growth. Nat Rev Cancer 2(1):38–47. 10.1038/nrc704 [PubMed: 11902584]
12. Heddleston JM, Li Z, Hjelmeland AB, Rich JN (2009) The hypoxic microenvironment maintains glioblastoma stem cells and promotes reprogramming towards a cancer stem cell phenotype. Cell Cycle 8(20):3274–3284 [PubMed: 19770585]

13. Keith B, Johnson RS, Simon MC (2012) HIF1α and HIF2α: sibling rivalry in hypoxic tumour growth and progression. Nat Rev Cancer 12(1):9–22. 10.1038/nrc3183
14. Yu T, Tang B, Sun X (2017) Development of inhibitors targeting hypoxia-inducible factor 1 and 2 for cancer therapy. Yonsei Med J 58(3):489. 10.3349/ymj.2017.58.3.489 [PubMed: 28332352]
15. Semenza GL, Agani F, Booth G et al. (1997) Structural and functional analysis of hypoxia-inducible factor 1. Kidney Int 51(2):553–555 [PubMed: 9027737]
16. Takeda N, O'Dea EL, Doedens A et al. (2010) Differential activation and antagonistic function of HIF-{alpha} isoforms in macrophages are essential for NO homeostasis. Genes Dev 24(5):491–501. 10.1101/gad.1881410 [PubMed: 20194441]
17. Gu YZ, Moran SM, Hogenesch JB, Wartman L, Bradfield CA (1998) Molecular characterization and chromosomal localization of a third alpha-class hypoxia inducible factor subunit, HIF3alpha. Gene Expr 7(3):205–213 [PubMed: 9840812]
18. Dengler VL, Galbraith MD, Espinosa JM (2014) Transcriptional regulation by hypoxia inducible factors. Crit Rev Biochem Mol Biol 49(1):1–15. 10.3109/10409238.2013.838205 [PubMed: 24099156]
19. Rey S, Schito L, Wouters BG, Eliasof S, Kerbel RS (2017) Targeting hypoxia-inducible factors for antiangiogenic cancer therapy. Trends Cancer 3(7):529–541. 10.1016/j.trecan.2017.05.002 [PubMed: 28718406]
20. Masoud GN, Li W (2015) HIF-1α pathway: role, regulation and intervention for cancer therapy. Acta Pharm Sin B 5(5):378–389. 10.1016/J.APSB.2015.05.007 [PubMed: 26579469]
21. Gatenby RA, Gillies RJ (2004) Why do cancers have high aerobic glycolysis? Nat Rev Cancer 4(11):891–899. 10.1038/NRC1478 [PubMed: 15516961]
22. Jain RK, Di Tomaso E, Duda DG, Loeffler JS, Sorensen AG, Batchelor TT (2007) Angiogenesis in brain tumours. Nat Rev Neurosci 8(8):610–622. 10.1038/NRN2175 [PubMed: 17643088]
23. Gatenby RA, Frieden BR (2004) Information dynamics in carcinogenesis and tumor growth. Mutat Res-Fundam Mol Mech Mutagen 568(2):259–273. 10.1016/j.mrfmmm.2004.04.018
24. Corbet C, Feron O (2017) Tumour acidosis: from the passenger to the driver's seat. Nat Rev Cancer 17(10):577–593. 10.1038/NRC.2017.77 [PubMed: 28912578]
25. Griffiths L, Stratford IJ (1998) The influence of elevated levels of platelet-derived endothelial cell growth factor/thymidine phosphorylase on tumourigenicity, tumour growth, and oxygenation. Int J Radiat Oncol Biol Phys 42(4):877–883. 10.1016/S0360-3016(98)00360-5 [PubMed: 9845114]
26. Shi Q, Le X, Wang B et al. (2001) Regulation of vascular endothelial growth factor expression by acidosis in human cancer cells. Oncogene 20(28):3751–3756. 10.1038/SJ.ONC.1204500 [PubMed: 11439338]
27. Hjelmeland AB, Wu Q, Heddleston JM et al. (2011) Acidic stress promotes a glioma stem cell phenotype. Cell Death Differ 18(5):829–840. 10.1038/CDD.2010.150 [PubMed: 21127501]
28. Wang YL, Yao J, Chakhoyan A et al. (2019) Association between tumor acidity and hypervascularity in human gliomas using pH-weighted amine chemical exchange saturation transfer echo-planar imaging and dynamic susceptibility contrast perfusion MRI at 3T. AJNR Am J Neuroradiol 40(6):979–986. 10.3174/AJNR.A6063 [PubMed: 31097430]
29. Yao J, Chakhoyan A, Nathanson DA et al. (2019) Metabolic characterization of human IDH mutant and wild type gliomas using simultaneous pH- and oxygen-sensitive molecular MRI. Neurooncology 21(9):1184–1196. 10.1093/NEUONC/NOZ078
30. Jonasch E, Donskov F, Iliopoulos O et al. (2021) Belzutifan for renal cell carcinoma in von Hippel-Lindau disease. N Engl J Med 385(22):2036–2046. 10.1056/NEJMOA2103425/SUPPL_FILE/NEJMOA2103425_DATA-SHARING.PDF [PubMed: 34818478]
31. Soni S, Padwad YS (2017) HIF-1 in cancer therapy: two decade long story of a transcription factor. Acta Oncol 56(4):503–515. 10.1080/0284186X.2017.1301680 [PubMed: 28358664]
32. Xia Y, Choi H-K, Lee K (2012) Recent advances in hypoxia-inducible factor (HIF)-1 inhibitors. Eur J Med Chem 49:24–40. 10.1016/j.ejmech.2012.01.033 [PubMed: 22305612]
33. Courtney KD, Infante JR, Lam ET et al. (2018) Phase I dose-escalation trial of PT2385, a first-in-class hypoxia-inducible factor-2α antagonist in patients with previously treated advanced clear cell renal cell carcinoma. J Clin Oncol 36(9):867–874. 10.1200/JCO.2017.74.2627 [PubMed: 29257710]

34. Li Z, Bao S, Wu Q et al. (2009) Hypoxia-inducible factors regulate tumorigenic capacity of glioma stem cells. Cancer Cell 15(6):501–513 [PubMed: 19477429]
35. Renfrow JJ, Soike MH, Debinski W et al. (2018) Hypoxia-inducible factor 2α: a novel target in gliomas. Future Med Chem 10(18):2227–2236. 10.4155/fmc-2018-0163 [PubMed: 30089425]
36. Renfrow JJ, Soike MH, West JL et al. (2020) Attenuating hypoxia driven malignant behavior in glioblastoma with a novel hypoxia-inducible factor 2 alpha inhibitor. Sci Rep 10.1038/S41598-020-72290-2
37. Wehn PM, Rizzi JP, Dixon DD et al. (2018) Design and activity of specific Hypoxia-Inducible Factor-2α (HIF-2α) inhibitors for the treatment of clear cell renal cell carcinoma: discovery of clinical candidate (S)-3-((2,2-Difluoro-1-hydroxy-7-(methylsulfonyl)-2,3-dihydro-1 H-inden-4-yl)oxy)-5-fluorobenzonitrile (PT2385). J Med Chem 61(21):9691–9721. 10.1021/acs.jmedchem.8b01196 [PubMed: 30289716]
38. Courtney K, Infante J, Lam E, et al. (2016) A phase I dose escalation trial of PT2385, a first-in-class oral HIF-2a inhibitor, in patients with advanced clear cell renal cell carcinoma In: ASCO Meeting Abstracts
39. Wallace EM, Rizzi JP, Han G et al. (2016) A small-molecule antagonist of HIF2a is efficacious in preclinical models of renal cell carcinoma. Ther Targets Chem Biol 76:5491–5500. 10.1158/0008-5472.CAN-16-0473
40. Johansson E, Grassi ES, Pantazopoulou V et al. (2017) CD44 interacts with HIF-2α to modulate the hypoxic phenotype of perinecrotic and perivascular glioma cells. Cell Rep 20(7):1641–1653. 10.1016/J.CELREP.2017.07.049 [PubMed: 28813675]
41. Nusblat LM, Tanna S, Roth CM (2020) Gene silencing of HIF-2α disrupts glioblastoma stem cell phenotype. Cancer Drug Resist 3(2):199. 10.20517/CDR.2019.96 [PubMed: 32566921]
42. Ellingson BM, Wen PY, Cloughesy TF (2017) Modified criteria for radiographic response assessment in glioblastoma clinical trials. Neurotherapeutics 14(2):307–320. 10.1007/s13311-016-0507-6 [PubMed: 28108885]
43. Ellingson BM, Bendszus M, Boxerman J et al. (2015) Consensus recommendations for a standardized Brain Tumor Imaging Protocol in clinical trials. Neuro-oncology 17(9):1188–1198. 10.1093/NEUONC/NOV095 [PubMed: 26250565]
44. Harris RJ, Cloughesy TF, Liau LM et al. (2015) pH-weighted molecular imaging of gliomas using amine chemical exchange saturation transfer MRI. Neuro-oncology 17(11):1514–1524. 10.1093/NEUONC/NOV106 [PubMed: 26113557]
45. Harris RJ, Yao J, Chakhoyan A et al. (2018) Simultaneous pH-sensitive and oxygen-sensitive MRI of human gliomas at 3 T using multi-echo amine proton chemical exchange saturation transfer spin-and-gradient echo echo-planar imaging (CEST-SAGE-EPI). Magn Reson Med 80(5):1962–1978. 10.1002/MRM.27204 [PubMed: 29626359]
46. Yao J, Ruan D, Raymond C et al. (2018) Improving B 0 correction for pH-weighted amine proton Chemical Exchange Saturation Transfer (CEST) imaging by use of k-means clustering and lorentzian estimation. Tomography 4(3):123–137. 10.18383/J.TOM.2018.00017 [PubMed: 30320212]
47. Xie C, Gao X, Sun D et al. (2018) Metabolic profiling of the novel hypoxia-inducible factor 2α inhibitor PT2385 in vivo and in vitro. Drug Metab Dispos 46(4):336–345. 10.1124/dmd.117.079723 [PubMed: 29363499]
48. Hirota T, Eguchi S, Ieiri I (2013) Impact of genetic polymorphisms in CYP2C9 and CYP2C19 on the pharmacokinetics of clinically used drugs. Drug Metab Pharmacokinet 28(1):28–37. 10.2133/dmpk.dmpk-12-rv-085 [PubMed: 23165865]
49. Courtney KD, Ma Y, de Leon AD et al. (2020) HIF-2 complex dissociation, target inhibition, and acquired resistance with PT2385, a first-in-class HIF-2 inhibitor, in patients with clear cell renal cell carcinoma. Clin Cancer Res 26(4):793–803. 10.1158/1078-0432.CCR-19-1459 [PubMed: 31727677]

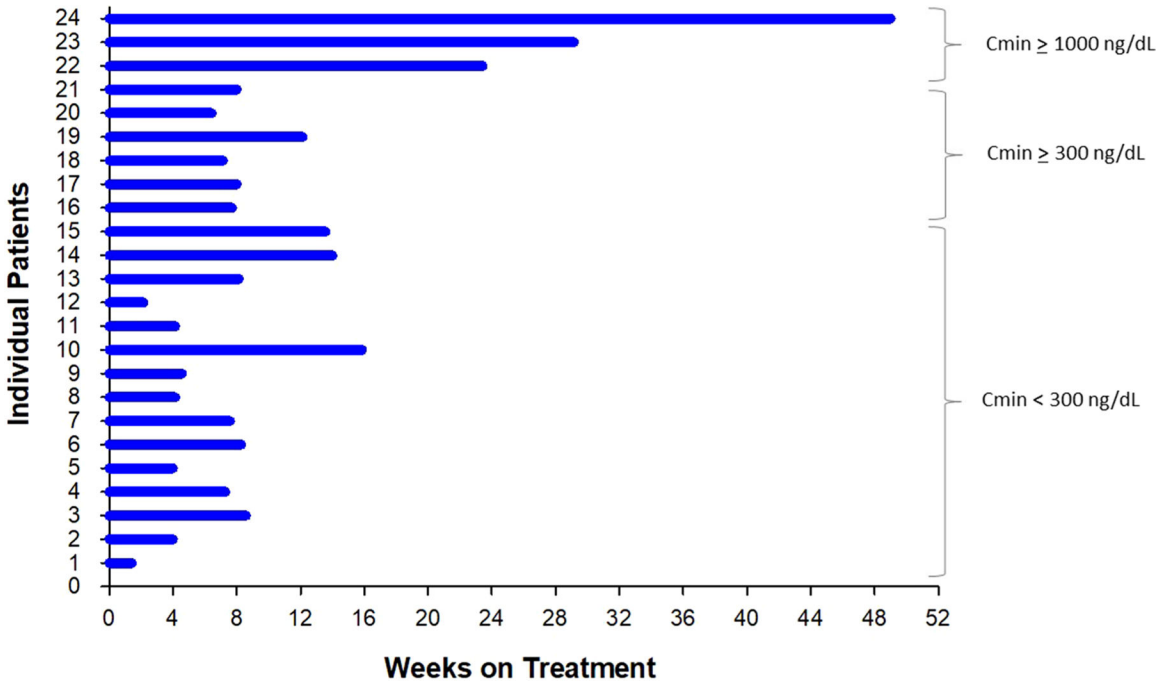

Fig. 1.

Swimmer's Plot Showing Duration on PT2385 Treatment for Patients with First Recurrent GBM. Weeks on treatment for all enrolled participants stratified by Day 15 C_{min}. demonstrating longer duration on treatment for patients with Day 15 C_{min} > 1000 ng/dL. C_{min} > 300 ng/dL estimated minimum target concentration for efficacy based on preclinical data

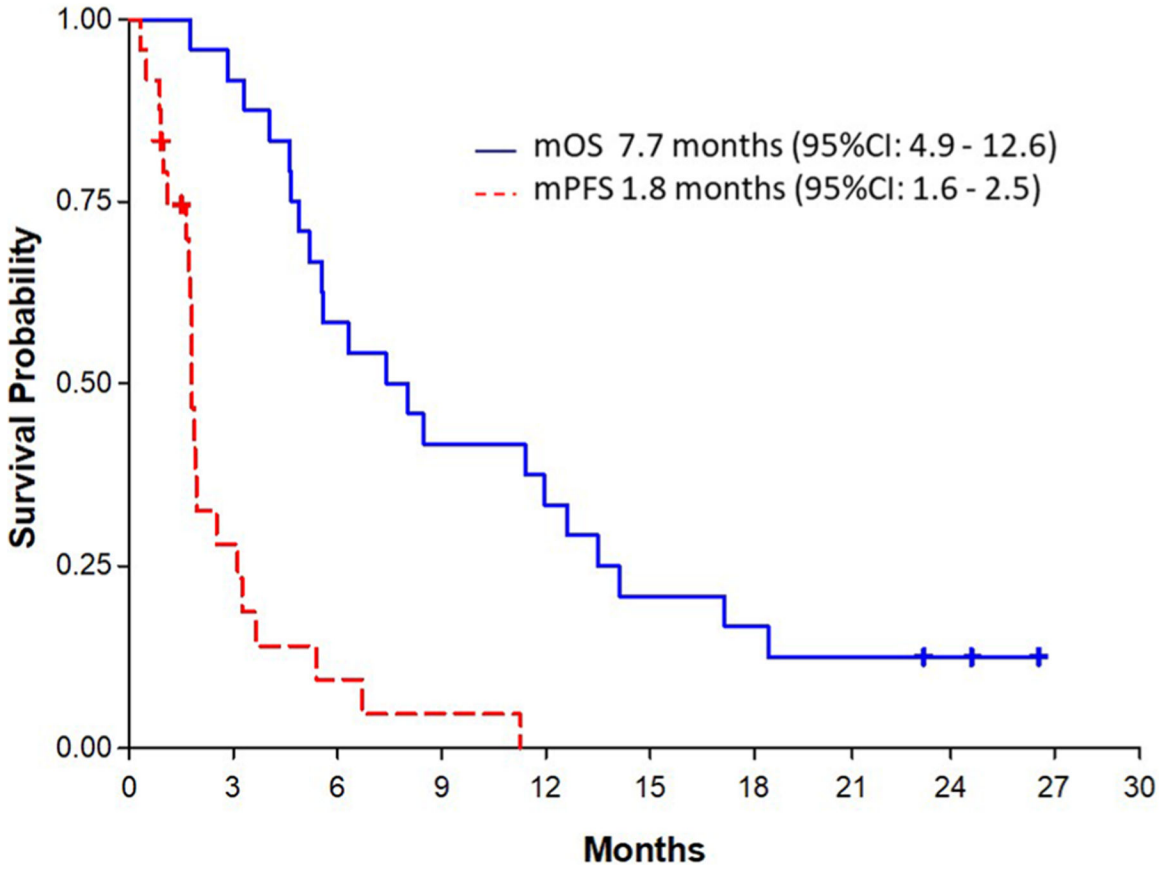

Fig. 2.

Kaplan–Meier Survival Curves for First Recurrent GBM Patients Treated with PT2385. Kaplan–Meier survival curves demonstrating a median overall survival of 7.7 months (95% confidence interval 4.9–12.6) and median progression-free survival of 2.7 months (95% CI 1.7–2.9)

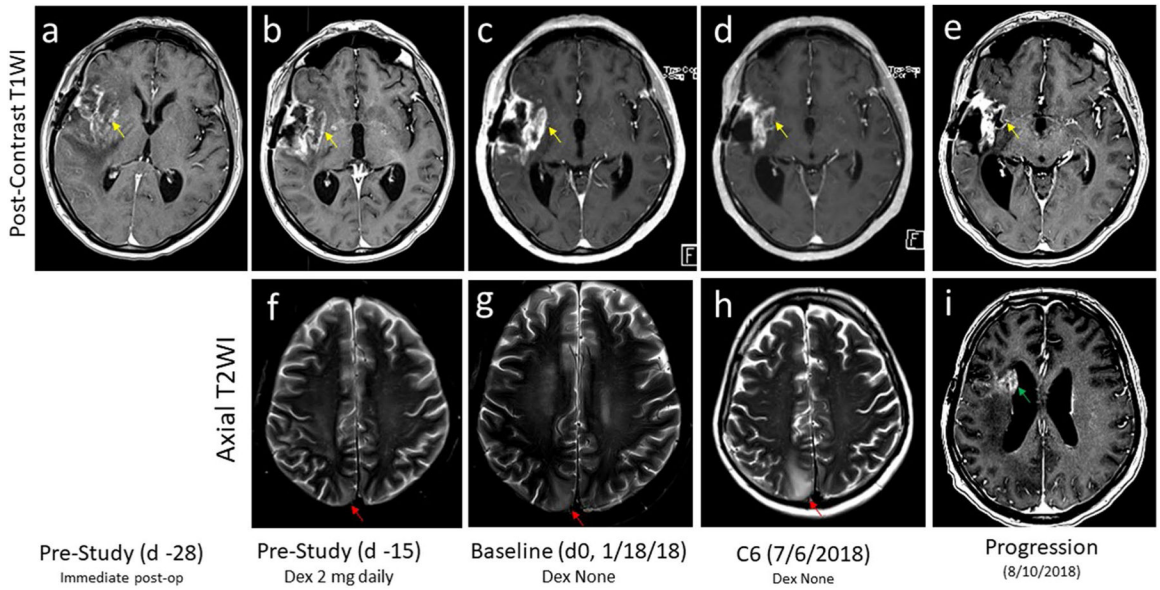

Fig. 3.

Representative MRI from Patient with High Systemic Drug Exposure to PT2385. Top (**a**–**e**) T1-weighted gadolinium enhanced axial MRI imaging showing residual contrast enhancing tumor in the right insular cortex (yellow arrows) in this patient with biopsy proven first recurrence of GBM; this right insular lesion demonstrates growth in the 28 days prior to study enrollment (day −28, **a**; to day 0, **c**) followed by stabilization on treatment (**d**). Bottom (**f**–**h**): T2-weighted axial images in this same patient showing a satellite non-enhancing site of infiltrative disease (red arrows) that did not respond to study drug treatment and progressively worsened on treatment. Progression in this patient was confirmed by a distant site of new contrast enhancing disease (**i**, green arrow)

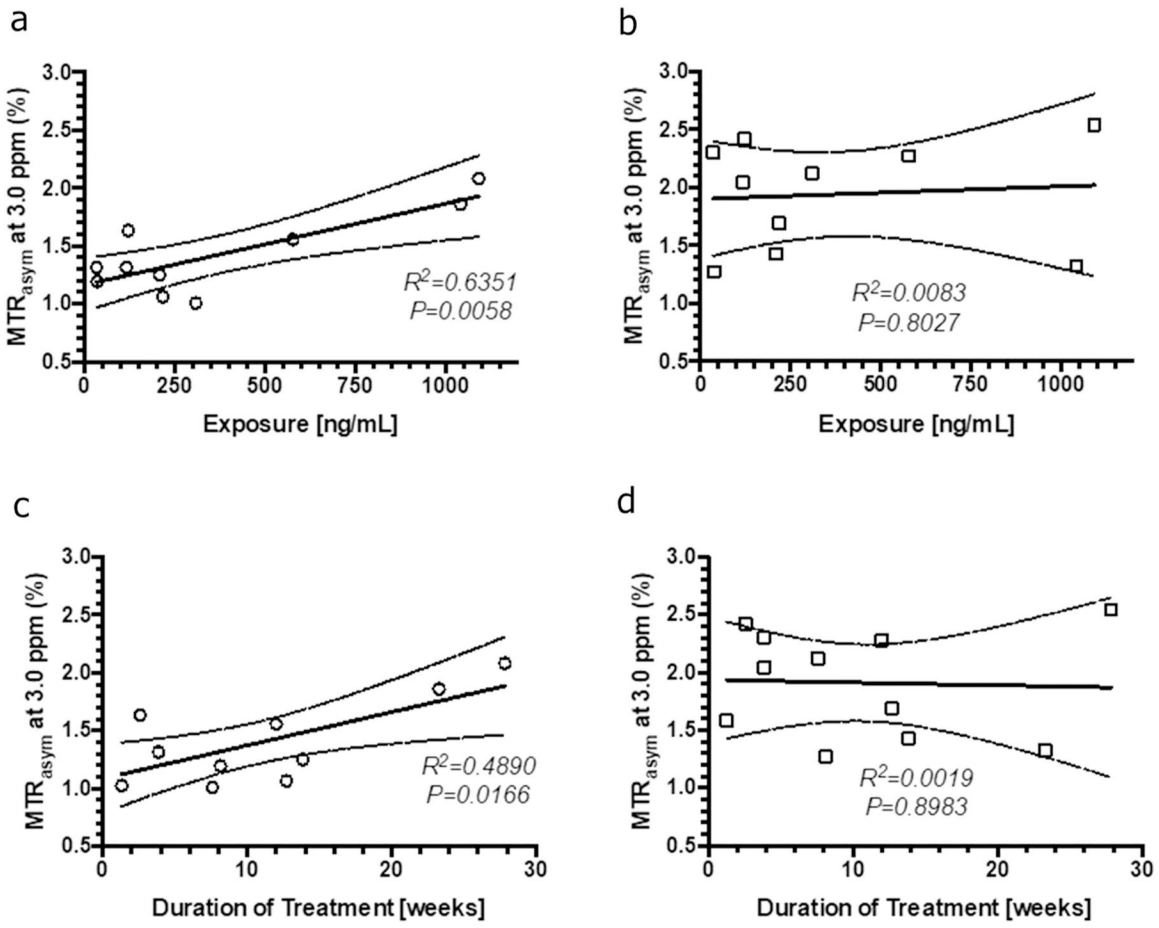

Fig. 4.

Baseline acidity correlated with duration of treatment within peritumoral non-enhancing and enhancing regions. Results of pH-weighted amine CEST imaging correlated with drug exposure (**a**, **b**) and duration of treatment (**c**, **d**). Higher values (on the y-axis) indicate increased acidity within peritumoral (**a**, **c**) and enhancing tissue (**b**, **d**) demonstrating a strong correlation between higher drug exposure and increased acidity in peritumoral tissue (**a**, $R^2 = 0.64$, $p = 0.0058$) but not enhancing tissue (**b**, $R^2 = 0.001$, $p = 0.81$). Similarly there is a moderate correlation between longer duration on treatment and increased acidity within peritumoral tissue (**c**, $R^2 = 0.49$, $p = 0.02$) but not enhancing tissue (**d**, $R^2 = 0.002$, $p = 0.90$). MTR_{asym}: MT Ratio (most commonly used CEST quantification metric)

Table 1

Clinical characteristics of the cohort

Characteristic	Categories	Value
Age (years, median, range)		62.1 (38.7–76.7)
Sex (n, % male)		15 (63%)
Race (n, %)	White	22 (92%)
	Black	1 (4%)
	Not reported	1 (4%)
MGMT promoter (n, %)	Methylated	11 (46%)
	Not methylated	12 (50%)
	Indeterminant	1 (4%)
Prior number of surgeries (median, range)		1 (1–3)
Extent of resection (n, %)	Gross total	14 (58%)
Karnofsky performance status (median, range)		80 (70–100)
Corticosteroid usage (n, %)		9 (38%)

J Neurooncol. Author manuscript; available in PMC 2024 February 13.

Table 2

CTCAE adverse events attributed to PT2385 as possible, probable or definite

Toxicity: possible, probable, or definite related to PT2385 (n = 24)	Grade 1 No. of patients (%)	Grade 2 No. of patients (%)	Grade 3 No. of patients (%)	Grade 4 No. of patients (%)	Total No. of patients (%)
Alanine aminotransferase increased	1 (4%)				1 (4%)
Alkaline phosphatase increased	1 (4%)				1 (4%)
Anemia	8 (33%)	3 (13%)	1 (4%)		12 (50%)
Confusion	2 (8%)	2 (8%)			4 (17%)
Dizziness	1 (4%)				1 (4%)
Dysphasia	2 (8%)				2 (8%)
Edema face	1 (4%)				1 (4%)
Edema limbs	2 (8%)				2 (8%)
Fall	1 (4%)				1 (4%)
Fatigue	6 (25%)	1 (4%)			7 (29%)
Flushing	1 (4%)				1 (4%)
Gait disturbance	1 (4%)				1 (4%)
Headache	1 (4%)				1 (4%)
Hyperglycemia	1 (4%)		1 (4%)		2 (8%)
Hyperkalemia	1 (4%)				1 (4%)
Hypermagnesemia	1 (4%)				1 (4%)
Hypocalcemia	1 (4%)				1 (4%)
Hypomagnesemia	1 (4%)				1 (4%)
Hyponatremia	2 (8%)		2 (8%)		4 (17%)
Hypophosphatemia	6 (25%)				6 (25%)
Hypoxia		1 (4%)	2 (8%)		3 (13%)
Lymphocyte decreased		2 (8%)		1 (4%)	3 (13%)
Muscle weakness	2 (8%)	2 (8%)			4 (17%)
Musculoskeletal & connective tissue disorder	1 (4%)	1 (4%)			2 (8%)
Nausea	4 (17%)	1 (4%)			5 (21%)
Neutrophil count decreased		1 (4%)			1 (4%)
Platelet count decreased	4 (17%)				4 (17%)
Pruritus	1 (4%)				1 (4%)

Toxicity: possible, probable, or definite related to PT2385 (n = 24)	Grade 1 No. of patients (%)	Grade 2 No. of patients (%)	Grade 3 No. of patients (%)	Grade 4 No. of patients (%)	Total No. of patients (%)
Seizure		1 (4%)			1 (4%)
Somnolence	1 (4%)				1 (4%)
Urinary incontinence	1 (4%)				1 (4%)
White blood cell decreased	1 (4%)	1 (4%)			2 (8%)

Table 3

Duration on treatment by day 15 C_{min}

Characteristic	Value	Value	Value
	PK < 300 ng/mL	PK 300–1000 ng/mL	PK ≥ 1000 ng/mL
N (%)	11 (55%)	6 (30%)	3 (15%)
Treatment duration (median weeks, 95% CI)	1.8 (0.9–3.1)	1.8 (1.6–5.2)	6.7 (5.4–11.3)

Day 15 C_{min} was not available for 4 study participants